

REPORT DOCUMENTATION PAGE

*Form Approved
OMB No. 0704-0188*

The public reporting burden for this collection of information is estimated to average 1 hour per response, including the time for reviewing instructions, searching existing data sources, gathering and maintaining the data needed, and completing and reviewing the collection of information. Send comments regarding this burden estimate or any other aspect of this collection of information, including suggestions for reducing the burden, to Department of Defense, Washington Headquarters Services, Directorate for Information Operations and Reports (0704-0188), 1215 Jefferson Davis Highway, Suite 1204, Arlington, VA 22202-4302. Respondents should be aware that notwithstanding any other provision of law, no person shall be subject to any penalty for failing to comply with a collection of information if it does not display a currently valid OMB control number.

PLEASE DO NOT RETURN YOUR FORM TO THE ABOVE ADDRESS.

1. REPORT DATE (DD-MM-YYYY) 03/18/2010	2. REPORT TYPE Reprint	3. DATES COVERED (From - To) 01 August 2009 - 06 December 2009
--	----------------------------------	--

4. TITLE AND SUBTITLE Low-dimensional Mott material: Transport in ultrathin epitaxial LaNiO3 films	5a. CONTRACT NUMBER W911-NF-09-1-0398
	5b. GRANT NUMBER
	5c. PROGRAM ELEMENT NUMBER

6. AUTHOR(S) Junwoo Son, Pouya Moetakef, James M. LeBeau, Daniel Ouellette, Leon Balents, S. James Allen, Susanne Stemmer	5d. PROJECT NUMBER
	5e. TASK NUMBER
	5f. WORK UNIT NUMBER

7. PERFORMING ORGANIZATION NAME(S) AND ADDRESS(ES) University of California, Santa Barbara, CA 93106, USA	8. PERFORMING ORGANIZATION REPORT NUMBER
---	---

9. SPONSORING/MONITORING AGENCY NAME(S) AND ADDRESS(ES) Army Research Office, Durham, NC 27703	10. SPONSOR/MONITOR'S ACRONYM(S) ARO
	11. SPONSOR/MONITOR'S REPORT NUMBER(S)

12. DISTRIBUTION/AVAILABILITY STATEMENT
Approved for public release; federal purpose rights

13. SUPPLEMENTARY NOTES

14. ABSTRACT
Electrical resistivity and magnetotransport are explored for thin 3–30 nm , epitaxial LaNiO3 films. Films were grown on three different substrates to obtain LaNiO3 films that are coherently strained, with different signs and magnitude of film strain. It is shown that d-band transport is inhibited as the layers progress from compression to tension. The Hall coefficient is “holelike.” Increasing tensile strain causes the film resistivity to increase, causing strong localization to appear below a critical thickness.

15. SUBJECT TERMS

16. SECURITY CLASSIFICATION OF:			17. LIMITATION OF ABSTRACT UU	18. NUMBER OF PAGES 3	19a. NAME OF RESPONSIBLE PERSON Susanne Stemmer
a. REPORT UU	b. ABSTRACT UU	c. THIS PAGE UU			19b. TELEPHONE NUMBER (Include area code) 825-893-6128

Reset

Low-dimensional Mott material: Transport in ultrathin epitaxial LaNiO₃ films

Junwoo Son,^{1,a)} Pouya Moetakef,¹ James M. LeBeau,¹ Daniel Ouellette,² Leon Balents,² S. James Allen,² and Susanne Stemmer^{1,b)}

¹Materials Department, University of California, Santa Barbara, California 93106-5050, USA

²Department of Physics, University of California, Santa Barbara, California 93106-5100, USA

(Received 6 December 2009; accepted 17 January 2010; published online 10 February 2010)

Electrical resistivity and magnetotransport are explored for thin (3–30 nm), epitaxial LaNiO₃ films. Films were grown on three different substrates to obtain LaNiO₃ films that are coherently strained, with different signs and magnitude of film strain. It is shown that *d*-band transport is inhibited as the layers progress from compression to tension. The Hall coefficient is “holelike.” Increasing tensile strain causes the film resistivity to increase, causing strong localization to appear below a critical thickness. © 2010 American Institute of Physics. [doi:10.1063/1.3309713]

Electron transport in two-dimensional systems has been extensively studied in normal metals and semiconductors. Recently, quantum confined films of strongly electron correlated materials have attracted renewed interest. For example, theory predicts dramatic changes in the magnetic and electronic properties for the confined “Mott material” LaNiO₃, including the possibility of high-temperature superconductivity.¹ Bulk rare-earth nickelates (*R*NiO₃ with *R*=rare earth cation), to which LaNiO₃ belongs, have been extensively researched because they exhibit a metal-insulator transition (MIT) that is a function of the radius of the rare-earth ion.² The transition is believed to be bandwidth-controlled and is associated with an expansion (contraction) of the unit cell.³ More recent investigations have shown that charge ordering also plays a role in the MIT of the nickelates.⁴ Unlike the other nickelates in the series, LaNiO₃ remains a paramagnetic metal at all temperatures, albeit a strongly correlated one.^{5,6} In this letter, we show that strong localization can be driven in LaNiO₃ films by a combination of strain and reduction in dimensionality.

Epitaxial LaNiO₃ films were grown by rf magnetron sputtering. Optimized growth parameters (100 mTorr total pressure, 600 °C substrate temperature) resulted in the smallest film lattice parameter and lowest resistivity. Films were grown on (001) surfaces⁷ of cubic (LaAlO₃)_{0.3}(Sr₂AlTaO₆)_{0.7} (LSAT), orthorhombic DyScO₃, and rhombohedral LaAlO₃. LaNiO₃ films [*a*=0.384 nm (Ref. 7)] on LSAT and DyScO₃ were under tensile strain and films on LaAlO₃ were under compressive strain (Table I). Film thicknesses were determined by cross-section transmission electron microscopy for which samples were prepared by mechanical wedge polishing only, as ion-milling damaged

the films. High-angle annular dark-field (HAADF) imaging was performed using a field emission scanning transmission electron microscope (FEI Titan 80–300). Hall bar structures with Ni/Au contacts were fabricated using photolithography and LaNiO₃ etching with hydrochloric acid. Temperature-dependent transport measurements were carried out using a physical property measurement system (Quantum Design). To obtain the Hall coefficient *R*_H, the Hall resistance *r*_H needed to be corrected for the magnetoresistance, i.e., *r*_H=[*V*_H(*B*)−*V*_H(−*B*)]/2*I*, where *V*_H(*B*) and *V*_H(−*B*) are the Hall voltages at positive and negative magnetic field *B*, respectively, and *I* is the current. The Hall coefficient was obtained from *R*_H=(∂*r*_H/∂*B*)*t*, where *t* is the film thickness.

All LaNiO₃ films were coherently strained up to 30 nm on LSAT and LaAlO₃ and up to 10 nm on DyScO₃. Figure 1(a) shows radial high-resolution x-ray diffraction scans through the 002 symmetric reflections of films and substrates. Thickness fringes indicate smooth and coherent films. The out-of-plane film lattice parameters reflect the film strain (Table I). Figure 1(b) shows HAADF images of a 3 nm thick LaNiO₃ film on LSAT, which confirmed the cube-on-cube epitaxial orientation relationship. All films are continuous.

Figure 2(a) shows the temperature-dependent resistivity of LaNiO₃ films on LSAT as a function of thickness. Thick (10–30 nm) films show metallic behavior with a resistivity of ~150 μΩ cm at room temperature, independent of film thickness. This value is comparable to the lowest reported values,^{6,8} indicating good oxygen stoichiometry.⁹ Below ~10 nm, the room temperature resistivity increases. The 4 nm films show a resistivity minimum at ~40 K [see inset in Fig. 2(a)] below which the resistivity scaled with log(*T*)

TABLE I. Substrate parameters and LaNiO₃ film properties on different substrates for 10 nm thick films.

Substrate	Lattice parameter (nm)	Lattice mismatch with LaNiO ₃ (%)	Measured out-of-plane film lattice parameter (nm)	$\partial\rho/\partial T _{250-300\text{ K}}$ (Ω cm K ⁻¹)	$\rho_0 _{2-80\text{ K}}$ (μΩ cm)	$A _{2-80\text{ K}}$ (μΩ cm K ⁻²)
LaAlO ₃	0.375	-1.32	0.3854	4.8×10^{-7}	46	1.9×10^{-3}
LSAT	0.387	0.78	0.3818	5.5×10^{-7}	60	2.2×10^{-3}
DyScO ₃	0.394	2.54	0.3779	1.3×10^{-6}	298	6.5×10^{-3}

^{a)}Electronic mail: json@mrl.ucsb.edu.

^{b)}Electronic mail: stemmer@mrl.ucsb.edu.

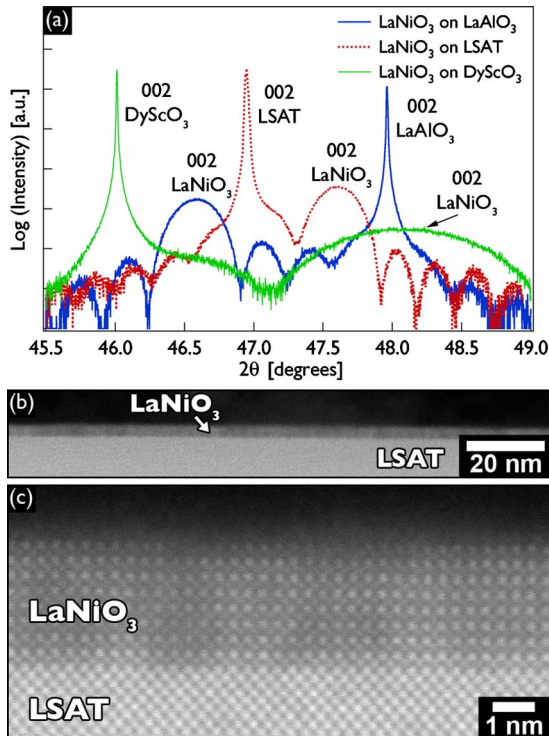


FIG. 1. (Color online) (a) High-resolution x-ray diffraction radial scans through the 002 reflections of LaNiO₃ films and LSAT, DyScO₃, and LaAlO₃ substrates, respectively. The film thickness were ~ 30 nm on LSAT and LaAlO₃ and 10 nm on DyScO₃, (b) Low-magnification, and (c) atomic resolution cross-section HAADF images of a 3 nm thick LaNiO₃ film on LSAT, showing a continuous film.

(see inset in Fig. 3). Further decrease in film thickness to 3 nm causes the films to become strongly localized (insulating), showing an increase in resistivity with decreasing temperature over the entire temperature range. For films on DyScO₃, which are under a larger tensile strain than those on LSAT, the transition to strong localization occurs at a larger thickness [Fig. 2(b)]. Independent of substrate, the critical thickness for strong localization of the tensile-strained films corresponds to a film resistance of ~ 10 k Ω/\square , the Mott minimum metallic conductivity as calculated from the Ioffe–Regel limit,¹⁰ where strong localization should appear. Compressive-strained LaNiO₃ films on LaAlO₃ show lower resistivities than films on LSAT and DyScO₃ and no MIT down to 2.5 nm. However, the thinnest (2.5 nm) film on LaAlO₃ also shows a resistivity minimum.

The observed resistivity minima and logarithmic temperature dependence in the intermediate regime can be due to weak localization^{11,12} or electron-electron interactions.¹³ Figure 3 shows that negative magnetoresistance in a perpendicular field is observed below the resistivity minimum. This is consistent with weak localization; a magnetic field suppresses the coherent interference needed for weak localization.¹¹ The Hall coefficient of LaNiO₃ layers on all substrates was positive, “holelike,” while the Seebeck coefficient was negative, similar to bulk LaNiO₃.^{6,9} A Fermi surface with any complexity can give rise to opposite signs.^{14,15} Band structure calculations and photoemission spectroscopy show small electron Fermi surfaces with an enhanced effective mass at the Γ point and a large hole Fermi surface around the R point.^{15,16} Figure 4 shows that R_H for films on LSAT and LaAlO₃ exhibits a strong temperature dependence, inconsistent with normal metallic behavior, which indicates

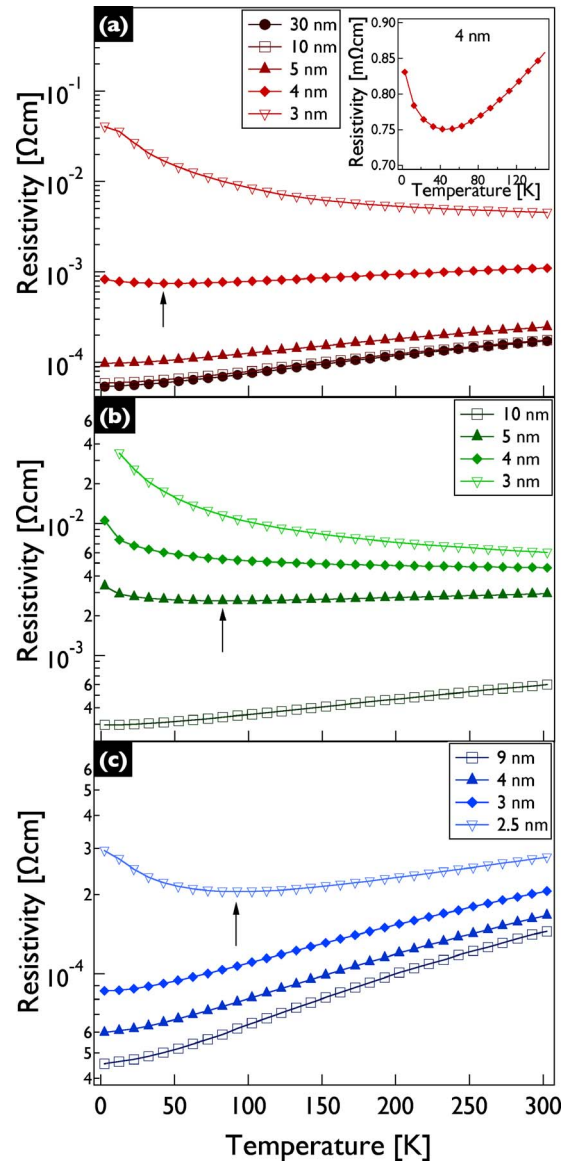


FIG. 2. (Color online) Temperature-dependence of the resistivity as a function of LaNiO₃ film thickness on (a) LSAT, (b) DyScO₃, and (c) LaAlO₃. The inset in (a) shows the data for the 4 nm film on a different scale to more clearly show the resistivity minimum at 40 K. The arrows show the resistivity minima for the weakly localized films on all three substrates. Below these thicknesses, films are strongly localized on LSAT and DyScO₃.

temperature-dependent scattering times and/or carrier concentrations/asymmetry.¹⁷ Because two carrier types with different mobilities are present, R_H cannot be easily converted into carrier concentrations.^{18,19}

At first glance the transport on the three substrates is similar: (i) metallic temperature dependence at room temperature for most thicknesses; (ii) emerging weak and then strong localization as the layer resistance approaches the Mott minimum conductivity, (iii) temperature dependent holelike R_H , and (iv) thickness dependent R_H , beyond the trivial $1/t$. Behind these similarities, a systematic trend toward localization or inhibited transport appears, which we will discuss next.

In the literature, thickness-dependent conductivity of metallic oxide thin films has been attributed to a “dead layer.”²⁰ We use the high temperature resistivity to explore thickness dependence and the potential role of dead layers. We use a phenomenological, classical description of the resistivity ρ

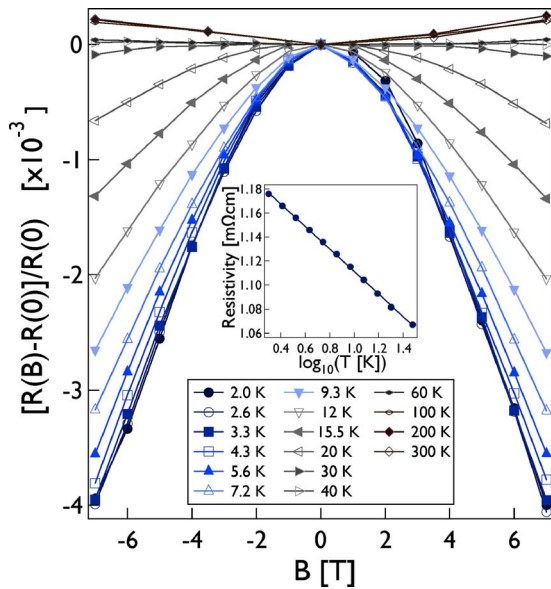


FIG. 3. (Color online) Normalized (to the zero-field value) resistance of the 4 nm LaNiO₃ film on LSAT as a function of applied magnetic field and temperature. The inset shows a logarithmic fit to the zero-field resistivity data as a function of temperature.

$$\rho = \left(\frac{m}{n}\right) \frac{1}{e^2} \left(\frac{1}{\tau_{\text{ph}}} + \frac{1}{\tau_{\text{surface}}} + \frac{1}{\tau_{\text{impurity}}} \right), \quad (1)$$

where e the electron charge, and the band structure is captured by the term that contains the carrier mass m and density n . The scattering rate is the sum of *temperature dependent*, intrinsic, phonon scattering (τ_{ph}), and *temperature independent* terms, such as surface/interface (τ_{surface}) and impurity (τ_{impurity}) scattering. The derivative of Eq. (1) with temperature, at high temperature, is given by

$$\frac{\partial \rho}{\partial T} = \left(\frac{m}{n}\right) \frac{1}{e^2} \frac{1}{\partial T} \left(\frac{1}{\tau_{\text{ph}}} \right). \quad (2)$$

Thus $\partial \rho / \partial T$ is independent of t , if the electrical thickness is equal to the measured thickness (no dead layer) and confinement does not produce changes in the band structure. For

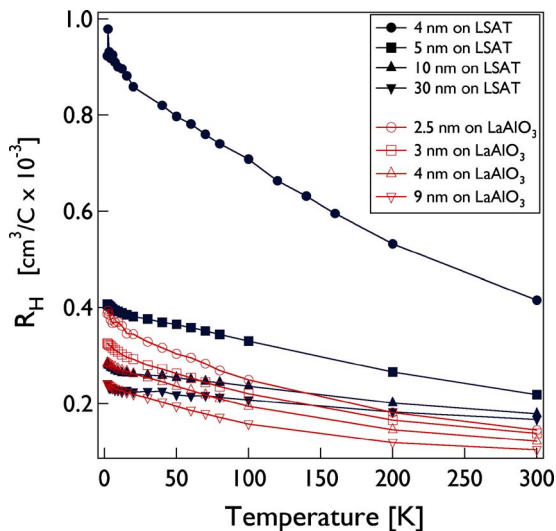


FIG. 4. (Color online) LaNiO₃ film Hall coefficient as a function of temperature and thickness on LSAT substrates (filled symbols) and LaAlO₃ (open symbols).

thick films on the same substrate, $\partial \rho / \partial T$ at room temperature is similar [see, i.e., Fig. 2(a)]; thus there is no need to invoke position dependent transport such as a “dead layer.” The thick film, low temperature (2–80 K), resistivity exhibits quadratic temperature dependence, $\rho = \rho_0 + AT^2$, characteristic of electron-electron interactions.⁵ Table I shows the coefficients A and ρ_0 , and the high temperature $\partial \rho / \partial T$ (250–300 K). Both A and $\partial \rho / \partial T$ are measures of changes in intrinsic transport as the biaxial strain evolves from compression to tension. Increasing $\partial \rho / \partial T$ is consistent with a narrowing of the d -band with tensile strain. Changes in d -band transport drive the films toward a localization transition. As the transport is inhibited the resistance reaches the two-dimensional Ioffe–Regel limit and strong localization sets in. Furthermore, although we are reluctant to over-interpret the Hall data, biaxial expansion may also reduce the effective number of carriers.

This work was supported by the MURI program of the Army Research Office (Grant No. W911-NF-09-1-0398). We thank Ram Seshadri, Nicola Spaldin, Sungbin Lee, and James Rondinelli for discussions and Oliver Bierwagen for help with the measurements. This work made use of the MRL facilities supported by the MRSEC Program of the NSF under Award No. DMR 05-20415.

¹P. Hansmann, X. P. Yang, A. Toschi, G. Khaliullin, O. K. Andersen, and K. Held, *Phys. Rev. Lett.* **103**, 016401 (2009).

²J. B. Torrance, P. Lacorre, A. I. Nazzari, E. J. Ansaldo, and C. Niedermayer, *Phys. Rev. B* **45**, 8209 (1992).

³J. L. García-Muñoz, J. Rodríguez-Carvajal, P. Lacorre, and J. B. Torrance, *Phys. Rev. B* **46**, 4414 (1992).

⁴U. Staub, G. I. Meijer, F. Fauth, R. Allenspach, J. G. Bednorz, J. Karpinski, S. M. Kazakov, L. Paolasini, and F. d’Acapito, *Phys. Rev. Lett.* **88**, 126402 (2002).

⁵K. Sreedhar, J. M. Honig, M. Darwin, M. Mcelfresh, P. M. Shand, J. Xu, B. C. Crooker, and J. Spalek, *Phys. Rev. B* **46**, 6382 (1992).

⁶K. P. Rajeev, G. V. Shivashankar, and A. K. Raychaudhuri, *Solid State Commun.* **79**, 591 (1991).

⁷We use the pseudocubic unit cells for denoting the surface orientations and lattice parameters for all noncubic substrates and the LaNiO₃ films.

⁸K. Tsubouchi, I. Ohkubo, H. Kumigashira, Y. Matsumoto, T. Ohnishi, M. Lippmaa, H. Koinuma, and M. Oshima, *Appl. Phys. Lett.* **92**, 262109 (2008).

⁹N. Gayathri, A. K. Raychaudhuri, X. Q. Xu, J. L. Peng, and R. L. Greene, *J. Phys.: Condens. Matter* **10**, 1323 (1998).

¹⁰N. F. Mott, *Philos. Mag.* **26**, 1015 (1972).

¹¹G. Bergmann, *Phys. Rep.* **107**, 1 (1984).

¹²P. A. Lee and T. V. Ramakrishnan, *Rev. Mod. Phys.* **57**, 287 (1985).

¹³B. L. Altshuler, A. G. Aronov, and P. A. Lee, *Phys. Rev. Lett.* **44**, 1288 (1980).

¹⁴S. Fujita and K. Ito, *Quantum Theory of Conducting Matter* (Springer, New York, 2007), p. 195.

¹⁵N. Hamada, *J. Phys. Chem. Solids* **54**, 1157 (1993).

¹⁶R. Eguchi, A. Chainani, M. Taguchi, M. Matsunami, Y. Ishida, K. Horiba, Y. Senba, H. Ohashi, and S. Shin, *Phys. Rev. B* **79**, 115122 (2009).

¹⁷N. Shirakawa, K. Murata, Y. Nishihara, S. Nishizaki, Y. Maeno, T. Fujita, J. G. Bednorz, F. Lichtenberg, and N. Hamada, *J. Phys. Soc. Jpn.* **64**, 1072 (1995).

¹⁸S. J. Allen, F. Derosa, C. J. Palmstrom, and A. Zrenner, *Phys. Rev. B* **43**, 9599 (1991).

¹⁹If magnetotransport can be measured in the regime where $\mu_{e,h}B > 1$, where $\mu_{e,h}$ is the respective carrier mobility, the Hall effect will be a nonlinear function of magnetic field and it may be possible to distinguish different carrier contributions, see Ref. 18. The layers explored here exhibit linear Hall effect and appear to be far from this limit.

²⁰J. Z. Sun, D. W. Abraham, R. A. Rao, and C. B. Eom, *Appl. Phys. Lett.* **74**, 3017 (1999).